Chatterjee, S. *et al.* (2014). *Géotechnique* **64**, No. 1, 83–88 [http://dx.doi.org/10.1680/geot.13.T.008]

TECHNICAL NOTE

A parkable piezoprobe for measuring c_v at shallow depths for offshore design

S. CHATTERJEE*, M. F. RANDOLPH* and D. J. WHITE*

The coefficient of consolidation (c_v) at shallow depth is an important parameter for the design of many offshore facilities, particularly pipelines. This paper sets out the concept, operation and interpretation of a new simple tool for measuring c_v in situ at shallow depths. This tool is a large cylindrical penetrometer with a hemispherical tip, which is embedded statically under self-weight, for example from a winch. After embedment, the tool is 'parked' – not requiring support from a drill-string – and the pore pressure dissipation is monitored. This 'parkable' feature allows the tool to be added to conventional drilling or penetrometer systems and used in parallel. The operation of the tool has been simulated using large-deformation finite-element analysis with the Cam Clay plasticity soil model. Results in the form of the normalised undrained penetration response and pore water pressure dissipation–time history are presented. The penetration response indicates the weight requirement of the device. The dissipation curves allow c_v to be determined from field measurements of pore pressure.

KEYWORDS: clays; consolidation; in situ testing; offshore engineering

INTRODUCTION

The rate of consolidation at shallow depth of subsea soils is an important parameter for the design of many offshore facilities, particularly pipelines. The design of on-bottom pipelines against axial movement requires correct estimation of the resistance between the pipe and the soil, which is controlled by the 'set-up' of effective stresses at the interface (Krost *et al.*, 2011; Chatterjee *et al.*, 2012b). There are other situations in which c_v at shallow depths is important, including assessments of the bearing capacity and settlement rate of shallow foundations.

The conventional method of estimating consolidation coefficient is through laboratory consolidation tests on undisturbed samples, or in the field, through dissipation stages during cone penetration tests (CPT), but these are difficult to interpret close to the soil surface.

This paper introduces a simple and low-cost alternative field tool, which is specifically focused on the determination of near-surface c_v. The tool is an elongated spheroid made of solid steel and instrumented with transducers to measure pore water pressure. The tool can be lowered into the seabed from a seabed-based site investigation system (Figure 1(a)), or could alternatively be lowered directly from a vessel in shallow water, or from a remotely operated vehicle (ROV). Seabed-based site investigation systems that integrate multiple tools into a single frame are an increasingly popular platform for offshore site investigations (e.g. Borel *et al.*, 2011; Kelleher *et al.*, 2011; Robertson *et al.*, 2012). While the seabed system is occupied with drilling, sampling and penetrometer testing, the new tool can, in parallel, log pore pressure dissipation data from which the value of coefficient

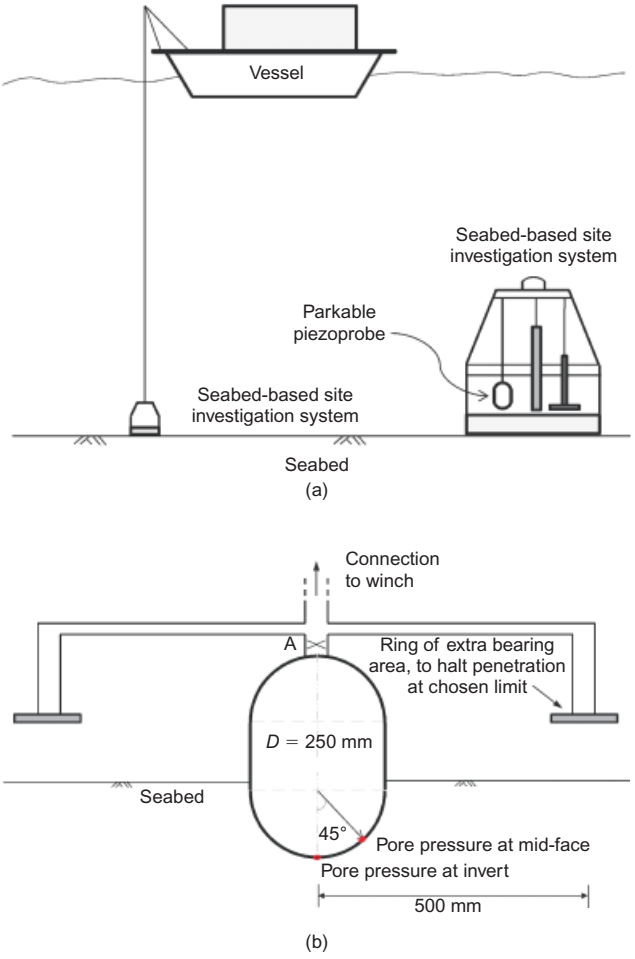

Fig. 1. (a) Seabed-based site investigation systems; (b) the parkable piezoprobe

Manuscript received 28 February 2013; revised manuscript accepted 2 July 2013. Published online ahead of print 17 October 2013. Discussion on this paper closes on 1 June 2014, for further details see p. ii.

* Centre for Offshore Foundation Systems, University of Western Australia, Crawley, Perth, Western Australia.

of consolidation (c_v) can be determined, providing an efficient use of vessel time.

The tool is termed a 'parkable piezoprobe' (PPP). In current practice, huge uncertainty exists in determining the value of c_v at shallow depths, because data are extrapolated from deeper CPT dissipation data, or are determined from laboratory tests, which are difficult to perform on very soft samples and can be unreliable. The aim of this device is to obtain more accurate values of c_v leading to a narrower design range. In addition, the device provides information on the shallow soil strength profile from the penetration stage.

Numerical analyses using a large-deformation finite-element (LDFE) methodology and the modified Cam Clay (MCC) soil model have been performed to study the penetration of the device and the consolidation–time history thereafter. Non-dimensional charts are provided that can be compared with the field data to estimate the value of c_v.

DEVICE DETAILS

A schematic diagram of the tool is shown in Figure 1(b). There is a cylindrical elongation in between two hemispheroids of 250 mm dia. (although the precise shape of the top is not important). The device is made of solid steel, making it heavy enough to statically self-penetrate up to 0·5 to one diameter in soft seabed conditions. It is envisaged that three or four pore water pressure transducers are located at the tip and at mid-face positions around a circle that subtends an angle of 45° from the axis of symmetry (Figure 1(b)). Measurement at the mid-face positions may prove advantageous, relative to the tip position where clogging of the transducer filter may occur.

The weight of the PPP can be optimised to accommodate the variations in seabed soil strength conditions. To increase the applicability of the device, an additional flat ring, located remote from the tool, can provide additional bearing area and halt the penetration of the device at the desired embedment (Figure 1(b)). The ring is shown at a distance of two times the diameter from the centre of the device to avoid interference with the stress and pore water pressure field of the central probe. The details of the weight requirement for different soil conditions are discussed later.

To deploy the device, it is lowered statically into the seabed from a winch. If the winch cable is equipped with a load cell this provides a load–penetration curve, from which the soil strength profile can be interpreted. Alternative arrangements such as a load cell immediately above the central probe (point A on Figure 1(b)) could be envisaged if the outer ring is used, to isolate the load applied to the central probe.

NUMERICAL DETAILS

The MCC soil constitutive model (Roscoe & Burland, 1968) was used with material parameters typical of a soft clay (Stewart, 1992; Chatterjee *et al.*, 2012b) (Table 1). An LDFE analysis methodology (Hu & Randolph, 1998), was used in the commercial finite-element software, Abaqus (Dassault Systèmes, 2011), as first implemented by Wang *et al.* (2010). The details of this methodology can be found in previous publications (Chatterjee *et al.*, 2012a, 2012b).

An axisymmetric model as shown in Figure 2 was developed using Abaqus. The interface between the PPP and the soil was modelled as a smooth contact. A permeable top boundary of the soil domain was assumed for pore pressure dissipation during the consolidation stage. Surcharges of 200 kPa and 1 kPa were applied on the top surface, as indicated on the right and left sides of Figure 2 respectively. These different values provide profiles of coefficient of consolidation (and shear strength) that were uniform and linearly increasing with depth respectively, using the same approach as Chatterjee *et al.* (2012b). The absolute values of s_u and c_v are irrelevant since the results are considered in normalised form throughout the paper.

The 1 kPa surcharge gives a profile in which c_v and s_u increase linearly from small values at the mudline ($c_{v,mudline}$ and $s_{u,mudline}$), reaching double the mudline value at a depth of approximately one diameter of the piezoprobe (meaning that the strength and c_v gradients k_{su} and k_{cv}, have dimensionless values of $k_{su}D/s_{u,mudline}$ and $k_{cv}D/c_{v,mudline} \sim 1$ for the 1 kPa surcharge case).

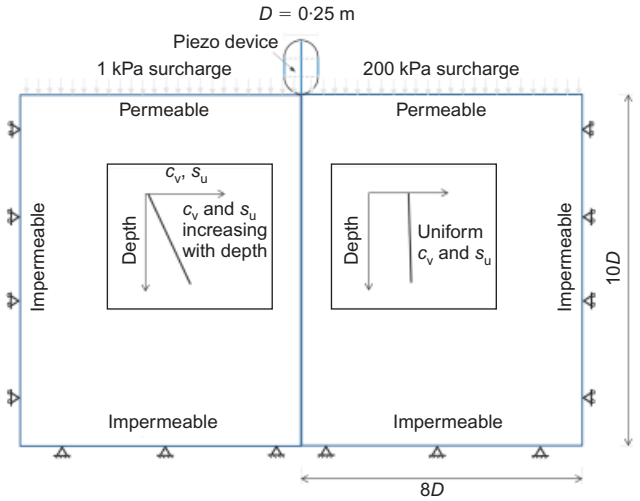

Fig. 2. Axisymmetric model used for numerical analysis

Table 1. Input numerical parameters

Parameter	Symbol	Value
Slope of critical state line (CSL) (angle of internal friction)	M (ϕ')	0·92 (23·5°)
Void ratio (at $p' = 1$ kPa on CSL)	e_{cs}	2·14
Slope of normal consolidation line	λ	0·205
Slope of swelling line	κ	0·044
Poisson ratio	μ	0·3
Saturated bulk unit weight	γ_{sat}	15 kN/m^3
Unit weight of water	γ_w	10 kN/m^3
Permeability of soil	k	1×10^{-9} m/s

UNDRAINED PENETRATION

In the analyses, the PPP was first penetrated statically to a depth of either 0·5D or 1D under undrained conditions. The penetration resistance was normalised by the equivalent triaxial undrained shear strength, s_u calculated following Wroth (1984) as described in Chatterjee *et al.* (2012b).

The undrained shear strengths calculated at the mudline are 0·248 kPa and 49·6 kPa for the 1 kPa and 200 kPa surcharges respectively. The normalised penetration responses for both cases are shown in Figure 3. The vertical resistance (V) plotted in Figure 3 is the geotechnical resistance after subtracting the buoyancy term from the total resistances and is given by

$$\left(\frac{V}{D^2 s_u}\right)_{\text{geotechnical}} = \left(\frac{V}{D^2 s_u}\right)_{\text{total}} - \frac{\gamma' v_{\text{sub}}}{D^2 s_u} \tag{1}$$

where the second term represents the soil buoyancy, with γ' the effective unit weight of the soil. For an embedment, w below the mudline, the submerged volume of the PPP is given by

$$\begin{aligned} v_{\text{sub}} &= \frac{\pi w^2}{3}(1{\cdot}5D - w) \quad \text{for} \quad w \leqslant 0{\cdot}5D \\ v_{\text{sub}} &= \frac{\pi D^3}{12} + \frac{\pi D^2}{8}(2w - D) \quad \text{for} \quad 0{\cdot}5D < w \leqslant D \end{aligned} \tag{2}$$

The normalised penetration response can be fitted by a simple exponential law equation. Two different equations for above and below thresholds of $V/(D^2 s_u)$ achieve reasonable fits, which are given by

$$\frac{w}{D} = x \exp\left[y\left(\frac{V}{D^2 s_u}\right)\right] \quad \text{for} \quad \frac{V}{D^2 s_u} > \lambda \tag{3a}$$

$$\frac{w}{D} = m\left(\frac{V}{D^2 s_u}\right) \quad \text{for} \quad \frac{V}{D^2 s_u} \leqslant \lambda \tag{3b}$$

The coefficients x, y, λ and m are given in Table 2 for both cases.

WEIGHT ADJUSTMENT

The ideal penetration depth for the PPP is 0·5D to 1D. Greater embedment weakens the geometric analogy with a pipeline and retards the dissipation rate, whereas shallower embedment may lead to poor contact around the device and unreliable dissipation data.

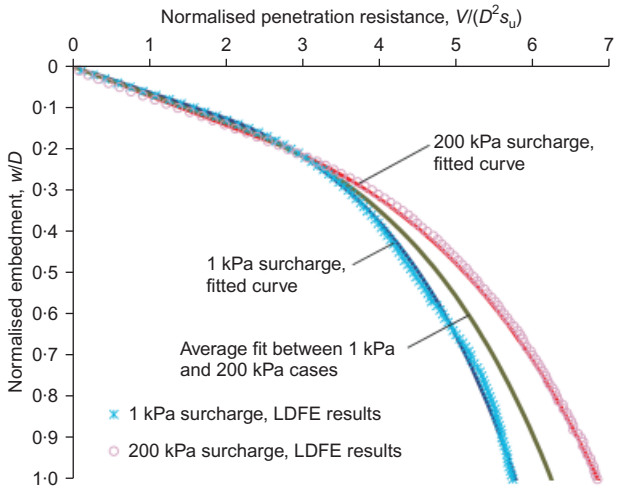

Fig. 3. Normalised penetration profiles for different soil strength cases

Table 2. Coefficients for penetration response model

Case	Surcharge	x	y	λ	m
Linear	1 kPa	0·042	0·55	1·9	0·063
Uniform	200 kPa	0·065	0·4	2·5	0·071
Average	Average fit	0·0535	0·47	2·2	0·068

Two bounding cases of shear strength profiles are studied in this paper. In reality, the shear strength gradient, k_{su} at the seabed can vary from $<$ 1 kPa/m to ~25 kPa/m, with the higher values generally associated with crustal features. At intermediate scales a mudline intercept of a few kPa is often indicated (Jeanjean *et al.*, 2005; Colliat *et al.*, 2011; Kuo & Bolton, 2013), but close inspection of the upper 0·5 m suggests that there is rarely any detectable true strength intercept at the mudline (DeJong *et al.*, 2013). For higher strength soils, the weight of the device may be insufficient to self-penetrate to the desired depth. To estimate the weight requirement for different soil strength profiles, an average curve using Equation 3 (coefficients shown in Table 2) has been fitted between the 1 kPa and the 200 kPa responses (i.e. linear and uniform soil strength) (Figure 3). The submerged weight required to achieve the desired displacement for different soil strength profiles has then been calculated using that curve (Figure 4(a)).

In the same figure, a straight line is shown indicating the submerged weight of the device if made of solid steel (neglecting internal voids for instrumentation wiring). In this case, it would penetrate under self-weight to a depth of at least 0·5D for any considered value of k_{su} if the mudline strength (s_{um}) is zero. For the device to penetrate to 1D depth, the value of k_{su} must be less than or equal to 10 kPa/m for $s_{um} = 0$. Sufficient penetration (to 0·5D) would not occur for a mudline strength intercept of $s_{um} = 3{\cdot}5$ kPa, unless additional weight was provided.

An alternative presentation of this information is shown in Figure 4(b), where the weight of the device is assumed to be the solid steel weight and different combinations of k_{su} and s_{um} are plotted. For self-penetration of the device to 1D depth, the required shear strength at the invert is ~2·5 kPa. A value of ~3·4 kPa will cause 0·5D embedment. As shown in the shaded portions in Figure 4(b), different combinations of k_{su} and s_{um} are possible for the device to penetrate to the desired depth under its self-weight. If the values of k_{su} and s_{um} lie outside the shaded portions, the weight of the device has to be adjusted according to the weight requirement as explained earlier. To widen the applicability of the device, the weight can be maximised and an additional supporting ring fitted as shown in Figure 1(b).

PORE WATER PRESSURE DISSIPATION

As the PPP is penetrated into the soil under undrained conditions, excess pore water pressure is generated. The excess pore pressure near the tool normalised by the value at the invert at 1D embedment is shown in Figure 5 for both 1 kPa and 200 kPa surcharge, immediately after undrained penetration. This generated excess pore pressure is allowed to dissipate under the full bearing capacity load. The normalised pore pressure dissipations ($= \Delta u/\Delta u_i$) at the invert and the mid-face are plotted against the non-dimensional time T ($= c_v t/D^2$) in Figure 6(a) for $w/D = 0{\cdot}5$ and $w/D = 1$. Here, Δu is the excess pore water pressure at time t and Δu_i is the initial excess pore pressure at the corresponding location. The value of c_v is the initial value calculated using

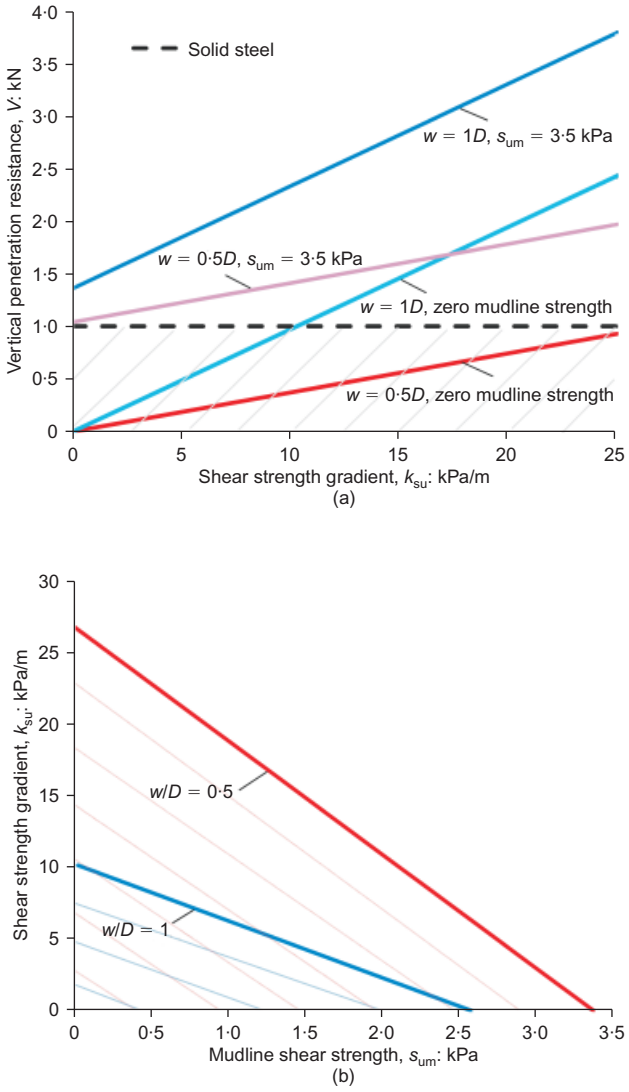

Fig. 4. (a) Weight requirements for self-penetration with varying soil strength gradient; (b) combinations of mudline strength and strength gradient required for self-penetration

$$c_v = \frac{k}{m_v \gamma_w} \tag{4}$$

The plastic isotropic volume compressibility, m_v can be expressed as

$$m_v = \frac{\lambda}{(1 + e_0)p_0'} \tag{5}$$

where e_0 is the initial void ratio and p_0' is the initial mean effective stress at a particular depth.

The dissipation–time histories show similar trends at the invert and the mid-face, although the dissipation is slightly faster at the mid-face for the initial period of consolidation. For the 200 kPa surcharge case, the variation of c_v is minimal with depth. So, the depth at which c_v is taken to calculate T is inconsequential. However, for the 1 kPa surcharge, c_v increases linearly with depth and the normalised dissipation curves depend on the depth chosen to calculate c_v. In Figure 6(a), c_v is taken as the initial value at the invert level for calculating T for the 1 kPa surcharge case and the dissipation curves are separated from those of the uniform c_v case. As shown in Figure 6(b), the dissipation curves for these two cases may be brought together if c_v is taken at a depth of 2·5–3·2 times the invert embedment for the linearly increasing c_v case. The c_v at these depths can be described as the 'operative' c_v. The ratio of the operative c_v to that at the invert, χ and the depth of the operative c_v for $w/D = 0{\cdot}5$ and 1 are shown in Table 3. It is seen that for both the cases the operative c_v is 1·76 times the c_v at the invert.

The dissipation–time history for the PPP is compared with conventional CPT dissipation responses calculated using the strain path method by Teh & Houlsby (1991), which assumes that the CPT is sufficiently deep not to be influenced by the soil surface. The dissipation curves for the CPT, PPP and a pipeline of the same diameter as the PPP (Chatterjee *et al.*, 2012b) are shown in Figure 6(c). The normalised pore pressure dissipation for the PPP is relatively faster than for the pipeline owing to its axisymmetric geometry, by a factor of 3–5. This shows that the PPP

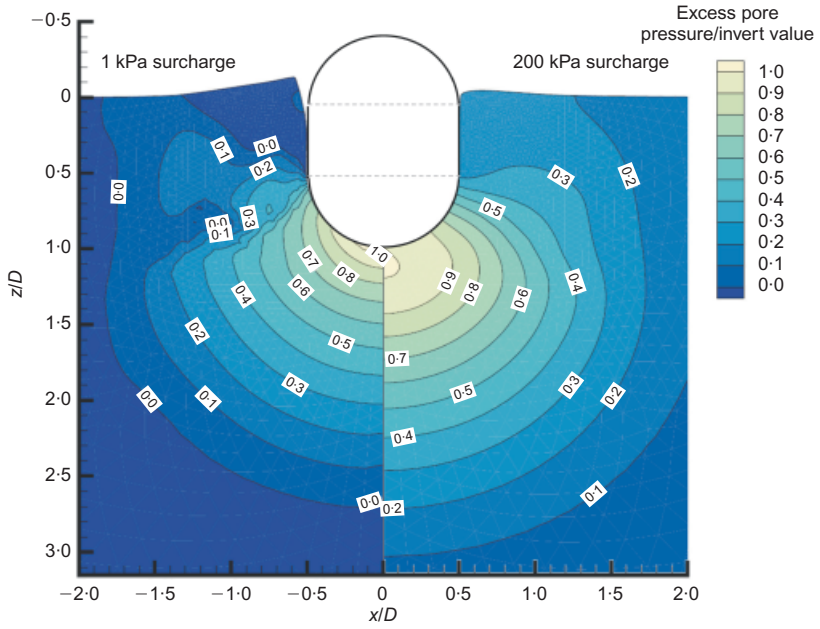

Fig. 5. Fields of initial excess pore pressure at 1*D* penetration

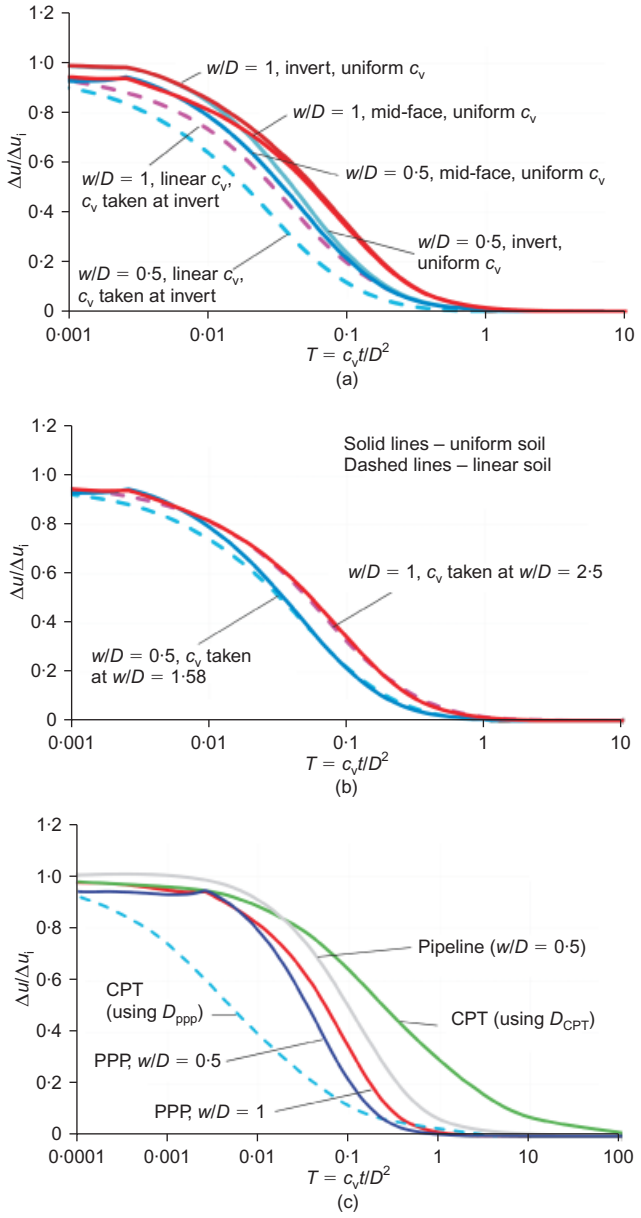

Fig. 6. Pore water pressure dissipation–time history: (a) c_v taken at the invert level for the 1 kPa surcharge case; (b) c_v taken at the operative depth for the 1 kPa surcharge case; (c) comparison with CPT and pipeline

Table 3. Linear case: operative c_v relative to uniform case

Initial embedment	$\chi = c_{v,operative}/c_{v,invert}$	Depth of operative c_v
$0{\cdot}5D$	1·76	$1{\cdot}58D$
$1D$	1·76	$2{\cdot}5D$

allows significantly more rapid determination of c_v compared to a pipe-shaped device of the same diameter.

The values T_{50} (non-dimensional time for 50% consolidation) and T_{90} (non-dimensional time for 90% consolidation) for the CPT, PPP and the pipe are shown in Table 4 for comparison. Using the PPP, T_{50} can be reached in a dimensionless time of 0·036 (for $w/D = 0{\cdot}5$), compared to 0·24 for the CPT. This factor of 7 difference reflects the influence of the free soil surface immediately above the PPP, which speeds up the rate of drainage.

If the dissipation curve for the CPT is scaled by the relative size compared to the PPP (to allow comparison of the elapsed time, t, to reach the same levels of consolidation), it shifts leftwards indicating faster determination of t_{50} (by a factor of about 7 for a 36 mm diameter cone) compared to the PPP. However, CPT data at shallow depths are potentially affected by the soil surface, so the theoretical dissipation curves are no longer reliable. Also, the PPP is designed to be used in parallel to a conventional penetrometer, so while the PPP dissipation is underway, in situ penetrometer tests can be conducted.

Table 4. Dimensionless dissipation times (uniform soil, using initial invert c_v)

Object		$T_{50} = c_v t_{50}/D^2$	$T_{90} = c_v t_{90}/D^2$
CPT ($D = 35{\cdot}7$ mm)		0·243	6·166
PPP ($D = 250$ mm)	$w/D = 0{\cdot}5$	0·036	0·180
	$w/D = 1{\cdot}0$	0·055	0·300
Pipe ($D = 250$ mm)		0·096	0·778

CONCLUDING REMARKS

This paper reports results of LDFE analyses performed to study the undrained penetration of a 'parkable piezoprobe' (PPP) and consequent dissipation of excess pore water pressure under constant load. The non-dimensional penetration curves assist in determining the weight required for the device to penetrate to the desired depth. The dissipation curves presented here can be compared with field data to compute c_v at shallow depths, which is a commonly required parameter for offshore design, particularly for pipelines. The main aim of this device is to reduce the uncertainty associated with the near-surface c_v.

The PPP described here is advantageous compared to other conventional methodologies for the following reasons.

1. The device is simple and straightforward to deploy independently from other offshore site investigation activities.
2. It can be piggybacked onto a conventional seabed-based site investigation system, requiring only a winch connection. It requires no other actuation, so can simultaneously log pore pressure data while the seabed system drills or performs other testing or sampling activities.
3. The rate of dissipation around the PPP is much greater than for a conventional pipeline of similar diameter, owing to the axisymmetric geometry. The dissipation is slower than around the smaller diameter cone penetrometer, but the dissipation data may be interpreted more reliably owing to the greater volume of soil involved in the process and explicit account of surface effects in the back-analysis.

ACKNOWLEDGEMENTS

This work forms the part of the activities of the Centre for Offshore Foundation Systems (COFS) at the University of Western Australia, currently supported as a node of the Australian Research Council Centre of Excellence for Geotechnical Science and Engineering and in partnership with the Lloyd's Register Foundation (LRF). LRF, a registered UK charity and sole shareholder of Lloyd's Register Group Ltd, invests in science, engineering and technology for public benefit, worldwide. Support through the Australian Research Council's Discovery and Fellowship programmes is also acknowledged. The third author acknowledges the support of Shell Development Australia.

NOTATION

c_v	coefficient of consolidation
$c_{v,mudline}$	coefficient of consolidation at mudline
D	diameter of the piezoprobe
e_0	initial void ratio
γ'	effective unit weight
k	permeability
χ	ratio of the operative c_v to that at the invert
k_{cv}	coefficient of consolidation gradient
k_{su}	shear strength gradient
m_v	plastic isotropic volume compressibility
p'_0	initial mean effective stress
s_u	undrained shear strength
$s_{u,mudline}$	undrained shear strength at mudline
T	non-dimensional time
T_{50}	non-dimensional time for 50% consolidation
T_{90}	non-dimensional time for 90% consolidation
t	time of consolidation
Δu	excess pore water pressure
Δu_i	initial excess pore pressure
V	vertical resistance
v_{sub}	submerged volume
w	piezoprobe invert embedment below mudline
x, y, λ, m	coefficients in equation (3)

REFERENCES

Borel, D., Puech, A. & Po, S. (2011). A site investigation strategy to obtain fast-track shear strength design parameters in deep water soils. *Proceedings of the 2nd international symposium on frontiers in offshore geotechnics*, Perth, Australia, pp. 253–258.

Chatterjee, S., Randolph, M. F. & White, D. J. (2012a). The effects of penetration rate and strain softening on the vertical penetration resistance of seabed pipelines. *Géotechnique* **62**, No. 7, 573–582, http://dx.doi.org/10.1680/geot.10.P.075.

Chatterjee, S., Yan, Y., Randolph, M. F. & White, D. J. (2012b). Elastoplastic consolidation beneath shallowly embedded offshore pipelines. *Géotechnique Lett*. **2**, No. 2, 73–79, http://dx.doi.org/10.1680/geolett.12.00031.

Colliat, J.-L., Dendani, H., Puech, A. & Nauroy, J.-F. (2011). Gulf of Guinea deepwater sediments: Geotechnical properties, design issues and installation experiences. *Proceedings of the 2nd international symposium on frontiers in offshore geotechnics*, Perth, Australia, pp. 59–86.

Dassault Systèmes (2011). *Abaqus analysis users' manual*. Providence, RI, USA: Simula Corp.

DeJong, J. T., Soga, K., Kavazanjian, E. *et al.* (2013). Biogeochemical processes and geotechnical applications: progress, opportunities and challenges. *Géotechnique* **63**, No. 4, 287–301, http://dx.doi.org/10.1680/geot.SIP13.P.017.

Hu, Y. & Randolph, M. F. (1998). A practical numerical approach for large deformation problems in soil. *Int. J. Numer. Analyt. Meth. Geomech*. **22**, No. 5, 327–350.

Jeanjean, P., Liedtke, E., Clukey, E. C., Hampson, K. & Evans, T. (2005). An operator's perspective on offshore risk assessment and geotechnical design in geohazard-prone areas. *Proceedings of the 1st international symposium on frontiers in offshore geotechnics*, Perth, Australia, pp. 115–143.

Kelleher, P., Low, H. E., Jones, C., Lunne, T., Strandvik, S. & Tjelta, T. I. (2011). Strength measurement in very soft upper seabed sediments. *Proceedings of the 2nd international symposium on frontiers in offshore geotechnics*, Perth, Australia, pp. 283–288.

Krost, K., Gourvenec, S. M. & White, D. J. (2011). Consolidation around partially embedded seabed pipelines. *Géotechnique* **61**, No. 2, 167–173, http://dx.doi.org/10.1680/geot.8.T.015.

Kuo, M. Y.-H. & Bolton, M. D. (2013). The nature and origin of deep ocean clay crust from the Gulf of Guinea. *Géotechnique* **63**, No. 6, 500–509, http://dx.doi.org/10.1680/geot.10.P.012.

Robertson, P. K., Gregg, J., Boyd, T. & Drake, C. (2012). Recent developments in deepwater investigations using a seafloor drill. *Proceedings of international conference on geotechnical and geophysical site characterization, Porto de Galinhas, Brazil*, vol. 4, pp. 1855–1859. London, UK: Taylor and Francis.

Roscoe, K. H. & Burland, J. B. (1968). On the generalised stress-strain behaviour of 'wet clay'. In *Engineering plasticity* (eds J. Heyman and F. A. Leckie), pp. 535–609. Cambridge, UK: Cambridge University Press.

Stewart, D. P. (1992). *Lateral loading of piled bridge abutments due to embankment construction*. PhD thesis, The University of Western Australia, Crawley, Perth, Western Australia.

Teh, C. I. & Houlsby, G. T. (1991). An analytical study of the cone penetration test in clay. *Géotechnique* **41**, No. 1, 17–34, http://dx.doi.org/10.1680/geot.1991.41.1.17.

Wang, D., White, D. J. & Randolph, M. F. (2010). Large deformation finite element analysis of pipe penetration and large-amplitude lateral displacement. *Can. Geotech. J.* **47**, No. 8, 842–856.

Wroth, C. P. (1984). The interpretation of in situ soil tests. *Géotechnique* **34**, No. 4, 449–489, http://dx.doi.org/10.1680/geot.1984.34.4.449.